



## Preparation and characterization of PE38KDEL-loaded anti-HER2 nanoparticles for targeted cancer therapy <sup>☆</sup>

Huaiwen Chen <sup>a</sup>, Jie Gao <sup>b</sup>, Ying Lu <sup>a</sup>, Geng Kou <sup>b,c</sup>, He Zhang <sup>a</sup>, Li Fan <sup>a</sup>, Zhiguo Sun <sup>a</sup>, Yajun Guo <sup>b,c,\*</sup>, Yanqiang Zhong <sup>a,\*</sup>

<sup>a</sup> Department of Pharmaceutical Science, College of Pharmacy, Second Military Medical University, 325 Guo He Road, Shanghai 200433, People's Republic of China

<sup>b</sup> International Joint Cancer Institute, Second Military Medical University, New Library Building West 10th-11th Floor, 800 Xiang Yin Road, Shanghai 200433, People's Republic of China

<sup>c</sup> Shanghai Center for Cell Engineering and Antibody, 399 Libing Road, Shanghai 201203, People's Republic of China

### ARTICLE INFO

#### Article history:

Received 2 December 2007

Accepted 11 March 2008

Available online 19 March 2008

#### Keywords:

Nanoparticles

PLGA

Immunotoxins

Targeted delivery

rhuMabHER2

### ABSTRACT

The clinical use of immunotoxins is severely limited by nonspecific toxicity. To overcome this limitation, PE38KDEL was used as a model protein toxin to prepare PE38KDEL-loaded poly(lactic-co-glycolic acid) (PLGA) antibody modified nanoparticles (NPs), which were covalently conjugated with Fab' fragments of a humanized anti-HER2 monoclonal antibody (rhuMabHER2) by a two-step carbodiimide method. The characterization of the PE38KDEL-loaded nanoparticles-anti-Fab' bioconjugates (PE-NPs-HER), such as particle size, zeta potential and morphology, were evaluated by dynamic light-scattering detector and transmission electron microscope (TEM). Micro BCA assay was used to determine the drug encapsulation efficiency and the quantity of Fab' conjugated with NPs. The binding affinity and internalization efficiency of PE-NPs-HER were demonstrated by flow cytometry and laser-scanning confocal microscopy. In comparison with PE38KDEL-loaded nanoparticles (PE-NPs) that lack anti-HER2 Fab', PE-NPs-HER had superior *in vitro* cytotoxicity against HER2-overexpressing breast cancer cell lines. Progressively, PE-NPs-HER has superior protective antitumor activity in HER2-overexpressing tumor-bearing mice than the control immunotoxin PE-HER constructed by chemically coupling PE38KDEL to rhuMabHER2. Most strikingly, in developed HER2-overexpressing tumor xenograft model, administration of PE-NPs-HER (0.9 mg/kg) showed a much better therapeutic efficacy in inhibiting tumor growth compared with PE-HER and other controls: final mean tumor load was  $13 \pm 6 \text{ mm}^3$  (mean  $\pm$  SD;  $n=8$ , significantly smaller than all other groups by ANOVA at 95% confidence interval). In addition, PE-NPs-HER were well tolerated in mice with a much higher MTD (maximally tolerated dose) than PE-HER (2.92 mg/kg vs. 0.92 mg/kg), indicating the systemic toxicity of PE38KDEL was dramatically reduced by PLGA encapsulation. Thus, the bioconjugates PE-NPs-HER may represent a potentially useful strategy for cancer therapy.

© 2008 Elsevier B.V. All rights reserved.

### 1. Introduction

Immunotoxins and ligand toxins are proteins used to treat cancer that are composed of antibody fragments or receptor ligands, respectively, linked to protein toxins. The immunotoxins and ligand toxins bind to a surface antigen on a cancer cell, enter the cell by endocytosis and kill it. Recently, there are about 30 kinds of immunotoxins and ligand toxins which have completed or are undergoing their clinical trials [1]. Some immunotoxins exhibited exciting therapeutic effect. For example, BL22, a stable disulfide-linked immunotoxin in which the Fv of the RFB4 antibody is fused to *Pseu-*

*domonas* exotoxin (PE), is the first agent that has been reported to induce a high rate of complete responses in hairy cell leukemia (HCL) patients that have resistance to purine analogues [2]. However, the use of immunotoxins in clinical trials has identified various limitations to their development [3]. One of the major limitations is nonspecific toxicity, which significantly reduces the amounts of immunotoxins that could be given to patients [2]. Nonspecific toxicity is usually characterized by damage to liver cells and vascular injury, which may be due to selective receptors for protein toxin on endothelial cells [4,5]. If nonspecific toxicity could be overcome, it should be possible to raise the dose of immunotoxins used to treat patients and obtain a better clinical response.

The use of biodegradable polymeric nanoparticles (NPs) designed to improve the pharmacological and therapeutic properties of drugs administered parenterally, may provide a practical means of reducing their toxic side effects [6–10]. Through polymerizer encapsulation, protein toxin could avoid the contact with receptors specific for protein toxins in normal tissues such as blood vessel, resulting in a

<sup>☆</sup> Note: Huaiwen Chen, Jie Gao and Ying Lu contributed equally to this work.

\* Corresponding authors. Zhong is to be contacted at Tel.: +86 21 25074591; fax: +86 21 25074591. Guo, International Joint Cancer Institute, Second Military Medical University, Shanghai, People's Republic of China. Tel.: +86 21 25070241; fax: +86 21 25074349.

E-mail addresses: [yguo\\_smmu@163.com](mailto:yguo_smmu@163.com) (Y. Guo), [yqzhong68@163.com](mailto:yqzhong68@163.com) (Y. Zhong).

decreased nonspecific toxicity. Furthermore, NPs can passively accumulate in tumors through a mechanism known as the enhanced permeability and retention (EPR) effect [6], and their biodistribution is largely determined by their physical and biochemical properties [11]. Notably, for targeted delivery, NPs could be surface functionalized with ligands such as antibody fragments and uptaken in a cell-specific manner [12–14]. By combining the tumor targeting properties of antibody fragments with the NPs, antibody modified NPs offer the promise of selective drug delivery to tumor cells, including internalization and intracellular drug release within targeted cells [15].

At present, diphtheria toxin (DT), PE and plant ribosome-inactivating proteins (RIPs) are used most frequently for preparation of immunotoxins [2]. PE38KDEL, a very potent toxin for preparation of immunotoxins, which we have obtained previously [16,17], was chosen as a model protein toxin in this study. In addition, poly(lactide-co-glycolide) (PLGA) polymer widely investigated for the controlled release of protein drugs, could be used to make antibody modified NPs, with terminal carboxylic acid groups reacting with amino group of antibody fragment to form stable amide linkage [18]. In this study, we developed PE38KDEL-loaded PLGA NPs targeting HER2 antigen (PE-NPs-HER), an important therapeutic target in breast cancer therapy [19]. PE-NPs-HER was constructed using Fab' fragments of a humanized anti-HER2 monoclonal antibody (rhuMab-HER2) [19], because the use of Fab' fragment would be helpful in providing better penetration of antibody modified NPs into solid tumors [20]. Meanwhile, as a control immunotoxin, PE-HER constructed by chemically coupling PE38KDEL to rhuMabHER2 was also developed as described before [21]. The present data show that PE-NPs-HER efficiently bound to and were internalized into HER2-overexpressing tumor cells, resulting in potent cytotoxicity compared with PE38KDEL-loaded NPs lacking anti-HER2 Fab'. Additionally, PE-NPs-HER had a reduced systemic toxicity and were well tolerated in mice with a higher maximally tolerated dose (MTD). Eventually, we describe the therapeutic potential of PE-NPs-HER in HER2-overexpressing breast cancer model.

## 2. Materials and methods

### 2.1. Materials

Poly(lactic-co-glycolic acid) (PLGA) (50:50, Resomer® RG503H, Mw=34,000) was obtained from Boehringer Ingelheim (Ingelheim, Germany). PVA (polyvinyl alcohol, Mw=25,000), 88% mole hydrolyzed was purchased from Aldrich Chemical Inc. (Munich, Germany). EDC (1-ethyl-3-(3-dimethylaminopropyl)-carbodiimide) and NHS (*N*-hydroxysuccinimide) were obtained from Sigma Chemical Co. (MO, USA). Micro BCA protein assay kit was obtained from Pierce Chemical Company (USA). RhuMabHER2 and humanized anti-CD25 mAb were kindly provided by the Shanghai Center for Cell Engineering and Antibody (Shanghai, China). Fab' fragments of rhuMabHER2 and anti-CD25 were prepared as described previously [22]. PE38KDEL was purified and analyzed as reported before [16]. Three human breast cancer cell lines BT-474, MDA-MB-231 and MCF-7 were maintained in the International Joint Cancer Institute, Second Military Medical University (Shanghai, China). All other chemicals were of analytical grade.

### 2.2. Preparation of antibody modified NPs

#### 2.2.1. Preparation of PE38KDEL-loaded PLGA NPs

The PE38KDEL-loaded PLGA NPs were prepared using a w/o/w emulsification solvent evaporation method as described by Blanco et al. [23]. Briefly, 150  $\mu$ l of an aqueous solution of PE38KDEL containing 10% (w/v) trehalose (Sigma, MO, USA) (w1) was emulsified in 1.5 ml of ethyl acetate containing 40 mg PLGA by sonication (Branson Sonicator® 450) for 60 s (100 W) in an ice bath to form the first

emulsion (w1/o). This w1/o emulsion was thereafter poured into 5 ml of 1% PVA solution (w2) and homogenized (POLYRON® PT-MA3100, Kinematica, Switzerland) for 1 min at 22,000 rpm to form double emulsion (w1/o/w2). The w1/o/w2 double emulsion was then diluted into 30 ml 0.3% PVA solution and stirred for 8 h to evaporate the ethyl acetate. The NPs were collected by centrifugation (L-100XP, Beckman, USA) at 50,000 rpm and washed thrice before lyophilization (V2K, Virtis, American). To fabricate fluorescein isothiocyanate (FITC) labeled PLGA NPs, FITC was conjugated to the terminal group of PLGA as reported previously [24]. Briefly, 0.7 mg 1,3-dicyclohexylcarbodiimide (DCC) and 0.4 mg NHS was added to 100 mg PLGA in 5 ml anhydrous methylene chloride. The mixture was stirred for 4 h, and the byproduct dicyclohexylurea was removed by filtration. The succinimidyl ester group of PLGA was converted to a primary amine group reacting with a 10-fold excess molar amount of 0.7 mg ethylenediamine in 5 ml methylene chloride. The reaction was carried out for 4 h, and then the product was purified by precipitation in an excess amount of cold diethyl ether and dried under vacuum overnight. FITC conjugated PLGA was produced by reacting 1.2 mg fluorescein isothiocyanate (dissolved in DMSO) to 50 mg primary amine terminated PLGA in 5 ml anhydrous DMSO. The sample was dialyzed against deionized water to remove unreacted FITC and lyophilized. There was no detectable change in molecular weight of PLGA after the FITC conjugation. FITC-PLGA NPs were prepared by blending PLGA and FITC conjugated PLGA at a 90/10 weight ratio and using a w/o/w emulsification solvent evaporation method as described above.

#### 2.2.2. NPs-anti-HER2 Fab' conjugation

PLGA-COOH was preactivated to its succinimide by using EDC and NHS, and then reacted with NH<sub>2</sub>-antibody fragment. Briefly, 1 ml of PLGA NPs suspension (~5 mg/ml in 10 mM NaH<sub>2</sub>PO<sub>4</sub>, pH 6.3) was incubated with 10  $\mu$ l of 50 mg/ml EDC and 10  $\mu$ l of 50 mg/ml NHS for 20 min at room temperature with gentle stirring. The resulting NHS-activated NPs were then covalently linked to Fab' fragments of rhuMabHER2 or anti-CD25 (1  $\mu$ g/ $\mu$ l in HEPES, pH 7.4). After the conjugation reaction, NPs were separated from free Fab' remaining by centrifugation (L-100XP, Beckman, USA) at 50,000 rpm  $\times$  5 min thrice. Finally, the Fab' fragments-NPs bioconjugates were washed and lyophilized. The following designations are used: PE-NPs (PE38KDEL-loaded PLGA nanoparticles), PE-NPs-HER (PE-NPs conjugated with anti-HER2 Fab' fragments), FITC-PE-NPs-HER (FITC FITC-labeled PE-NPs-HER), PE-NPs-anti-CD25 (PE-NPs conjugated with anti-CD25 Fab' fragments), FITC-PE-NPs-anti-CD25 (FITC FITC-labeled PE-NPs-anti-CD25). Drug-free PLGA nanoparticles conjugated with anti-HER2 Fab' are designated as NPs-HER. Additionally, the control immunotoxin PE-HER (PE38KDEL:rhuMabHER2=1:1 molar ratio) was constructed by chemically coupling PE38KDEL to rhuMabHER2 as described before [21].

### 2.3. Characterization of antibody modified NPs

#### 2.3.1. Particle size, zeta potential, morphology

Freeze-dried NPs were dispersed in deionized water (pH=7.0). Average size and zeta potential of PE-NPs and PE-NPs-HER were analyzed using a dynamic light-scattering detector (Zeta sizer 3000HS, Malvern, UK). At least three different batches were analyzed to give an average value and standard deviation for the particle diameter and zeta potential. The morphological examination of PE-NPs-HER was performed by transmission electron microscope (TEM). Briefly, after the PE-NPs-HER were lyophilized, the dried NPs were resuspended with deionized water. Samples were prepared by dropping one drop of dilute dispersion onto a copper grid coated with a carbon membrane. The surface morphology of the PE-NPs-HER samples was then visualized under the JEOL 2010 TEM (accelerating voltage of 200 kV).

### 2.3.2. Evaluation of drug contents

Drug loading determination was carried out as following: 20 mg of PE-NPs was dispersed in 10 ml of 0.04 M NaOH/2.5% SDS solution and kept in an orbital shaker at constant gentle shaking of 110 rpm at 37 °C for 24 h to hydrolyze the NPs. The weight ratios of PE38KDEL to NPs were determined by measuring the amount of PE38KDEL using a Micro BCA assay kit, as described before [25]. The encapsulation efficiency of PE38KDEL was determined by ratio of the actual amount of encapsulated protein over the total amount of protein used for the preparation of the NPs.

### 2.3.3. Determination of anti-HER2 Fab' on the surface of NPs

The following methods were used to confirm anti-HER2 Fab' on the NPs surface:

**2.3.3.1. Flow cytometry.** A dispersion of NPs conjugated with FITC FITC-labeled anti-HER2 Fab' was introduced directly into a flow cytometer and analyzed using FAC Scan flow cytometer (Becton Dickinson, San Jose, CA) as described before [26]. As a control, un-conjugated NPs were also analyzed.

**2.3.3.2. Laser-scanning confocal microscopy.** FITC FITC-labeled NPs conjugated with phycoerythrin labeled anti-HER2 Fab' were re-dispersed in phosphate-buffered saline (PBS) at pH 7.4. The localization of FITC and phycoerythrin was observed with Leica TCS SP2 Confocal Spectral Microscope (UV-VIS). FITC FITC-labeled NPs were run as a control and the images were analyzed with the Leica Confocal Software.

**2.3.3.3. Protein assay.** The amount of bound Fab' onto NPs surface was quantified by the Micro BCA method as previously described [25,26]. 500  $\mu$ l of Micro BCA working solution was added to 500  $\mu$ l PBS (pH=7.0) dispersion of NPs of PE-NPs-HER (1 mg/ml) and PE-NPs (1 mg/ml, served as blank) respectively, after 60 min of incubation, the absorbance was measured at 562 nm using a microplate reader (FLx800TB, Bio Tek, USA). The results were compared to a standard curve of Fab' solution in PBS (pH=7.0) ranged from 0.5  $\mu$ g/ml to 20  $\mu$ g/ml.

## 2.4. In vitro experiments

### 2.4.1. Cell culture

Three human breast cancer cell lines BT-474, MDA-MB-231 and MCF-7 were cultivated in monolayers to 80% confluence in RMPI 1640 medium supplemented with 10% fetal bovine serum at 37 °C in humidified environment of 7.5% CO<sub>2</sub>. The medium was replenished every other day and the cells were subcultured after reached confluence.

### 2.4.2. Recognition properties of antibody modified NPs

To examine the binding ability of antibody modified NPs to BT-474, MDA-MB-231 and MCF-7 cells,  $1 \times 10^6$  cells were treated with various concentrations (0–1000  $\mu$ g/ml) of rhuMAbHER2 for 30 min at 4 °C, before incubation with 1 mg FITC-PE-NPs-HER in 1 ml culture medium for 60 min at 37 °C, then cells were pelleted by centrifugation. Thereafter, the cells were then washed and analyzed by flow cytometry analysis (FCM). FCM was performed using a FAC Scan flow cytometer (Becton Dickinson, San Jose, CA).

### 2.4.3. Binding and internalization of antibody modified NPs

Binding and internalization of FITC FITC-labeled NPs in HER2-overexpressing and negative cell lines were examined by LSCM. BT-474 and MCF-7 cells were incubated with the NPs for 5 min, 2 h at 37 °C respectively, and then washed twice with PBS followed by fixation with 4% *p*-formaldehyde (PFA) for 30 min. Afterwards, DAPI (Invitrogen) was used to counterstain the nuclei of the cells. Finally, cells were imaged by Leica TCS SP2 Confocal Spectral Microscope (UV-VIS) and the images were analyzed with the Leica Confocal Software.

### 2.4.4. In vitro cytotoxicity

Cytotoxicity was analyzed using Cell Titer 96 non-radioactive cell proliferation assay kit according to the manufacturer's protocol (Promega, Madison, WI) [17]. Briefly, breast cancer cells ( $1 \times 10^4$ ) were cultured in the presence or absence of PE38KDEL-loaded NPs, PE-HER or free PE38KDEL for 2 days at 37 °C in a CO<sub>2</sub> incubator. The concentrations of PE38KDEL used in this assay were varied from 1 to 20,000 pM (equivalent to PLGA concentration of up to 0.13 mg/ml). Cytotoxicity of NPs and NP-HER without PE38KDEL was evaluated at 2 days at the highest PLGA concentration (0.13 mg/ml) used in the cytotoxicity assays. Then, 20  $\mu$ l of MTS/PMS solution was added to each well. After incubation for 2 h at 37 °C, the absorbance of each well was measured at 490 nm using a microplate reader.

## 2.5. In vivo experiment

### 2.5.1. Nonspecific toxicity assay

BALB/c nude mice were obtained from the Planned Parenthood Research Institute, Shanghai, People's Republic of China and maintained in a pathogen-free condition according to guideline of the Committee on Animals of the Second Military Medical University. For MTD studies, BALB/c nude mice were injected s.c. with  $5 \times 10^6$  BT-474 cells. Once tumors size reached 200 to 300 mm<sup>3</sup>, animals were treated with various doses of PE38KDEL, PE-HER, PE-NPs, or PE-NPs-HER (10 mice/group). Treatments were administered through the tail vein over three weekly doses. Total PE38KDEL administered ranged from 0.45 to 4.5 mg/kg. Mice were monitored for weight and gross toxicity as described over 2 months, the typical duration of the therapy studies. The MTD was defined as the highest tested dose that gave <20% weight loss and no treatment-related deaths. Furthermore, liver damage was also assessed in the above BALB/c nude mice bearing breast tumor by measuring plasma enzyme activity of alanine aminotransferase (ALT) determined using an automated procedure as described before [27]. Mice were euthanized 72 h after injection of drugs through the tail vein. Liver were fixed by 4% paraformaldehyde. Sections from liver were stained with hematoxylin and eosin (H&E) and examined histologically.

### 2.5.2. In vivo antitumor study

Antitumor activity of various agents was determined in BALB/c nude mice bearing human breast cancer. For protective experiments, groups of 8 nude mice were s.c. inoculated on the back with  $5 \times 10^6$  BT-474 cells on day 0. Starting on day 1, mice were injected with various agents through the tail vein twice daily for three consecutive days. Tumors were measured with a caliper every 5 days for an additional 60 days and tumor volume was calculated using the following formula: tumor volume (mm<sup>3</sup>) = [length  $\times$  (width)<sup>2</sup>]/2. On day 60, the tumor development was evaluated by palpation, autopsy, and tissue staining (Supplementary Fig. 4), and the number of tumor-bearing mice of each group was calculated.

For therapeutic experiments, tumor growth was induced by s.c. injection of  $5 \times 10^6$  BT-474 cells on the back. After 20 days when the tumor growth was visible (about ~50 mm<sup>3</sup>), mice were injected with various agents through the tail vein twice daily for three consecutive days. Tumors were measured with a caliper every 5 days for an additional 60 days and tumor volume was calculated as described above. In addition, one-way ANOVA with Dunnett's post-test for multiple

**Table 1**  
Size and zeta potentials of various NPs

	Drug-free NPs	PE-NPs	PE-NPs-HER
Size	105.0 $\pm$ 11.5 nm <sup>a</sup>	108.3 $\pm$ 13.9 nm	124.2 $\pm$ 21.2 nm
Zeta potential	-25.2 $\pm$ 1.4 mV	-36.2 $\pm$ 5.3 mV	12.0 $\pm$ 7.4 mV

<sup>a</sup> Data are expressed as the mean  $\pm$  SD ( $n = 10$ ).

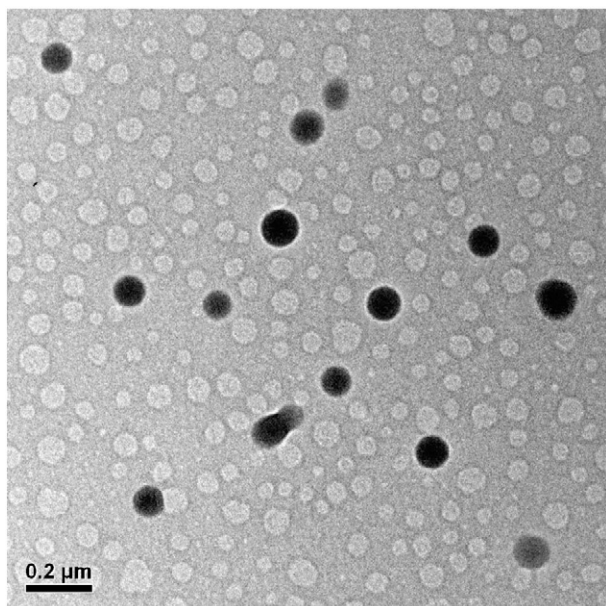


**Fig. 1.** Representative transmission electron microscope (TEM) image of resulting PE-NPs-HER is shown. Size bar indicates 0.2  $\mu\text{m}$ .

comparisons was used to compare treatment effects of each group for tumor size at the end end-point (day 80).

### 3. Results and discussion

#### 3.1. Characterization of NPs

##### 3.1.1. Particle size, zeta potential, morphology

NPs were prepared from a PLGA polymer containing free carboxylic end groups, using a modified double emulsion solvent evaporation

method. As the size of the NPs is important for establishing drug delivery strategies to specific sites of the body, the smaller NPs ( $\sim 100$  nm) may be prone to minimize the particle uptake by nontargeted cells, including their premature clearance by the MPS (mononuclear phagocytic system) [28]. The resulting PE-NPs were sized at  $108.3 \pm 13.9$  nm (mean  $\pm$  SD;  $n=10$ ) (Table 1 and Supplementary Fig. 1), which was not much larger than drug-free NPs ( $P>0.05$ ). However, there was about 16 nm increase in the particle size of PE-NPs-HER, presumably owing to the presence of anti-HER2 Fab' fragments on the NPs surface. The mean zeta potential of NPs was  $-25.2 \pm 1.4$  mV (mean  $\pm$  SD;  $n=10$ ), indicating that some free carboxylic end groups of the polymer were located on the surface of NPs. The encapsulation of negatively charged PE38KDEL into NPs resulted in a more negative surface charge, which may increase nonspecific interaction of the positively charged anti-HER2 Fab' with the PE-NPs. As the mean zeta potential of PE-NPs-HER exhibited a positive value of  $12.0 \pm 7.4$  mV (mean  $\pm$  SD;  $n=10$ ), we further concluded that the increase in zeta potential may be attributed to the presence of Fab' on the NPs surface. As shown in Fig. 1, PE-NPs-HER appeared spherical in shape, with a relatively monodispersed size.

##### 3.1.2. Evaluation of drug contents

We had optimized formulations to control the size of NPs as described above. Furthermore, drug contents also play a critical role in targeted drug delivery. To obtain large drug loading to meet therapeutic needs, high concentration of PE38KDEL ( $\approx 4$  mg/ml, the solubility of PE38KDEL was about 10 mg/ml) was chosen as the concentration of inner water phase. The prepared PE-NPs with a drug loading of  $8.5 \pm 0.2$   $\mu\text{g}/\text{mg}$  (mean  $\pm$  SD;  $n=4$ ) and an encapsulation efficiency of  $41.8 \pm 2.3\%$  (mean  $\pm$  SD;  $n=4$ ) was used in subsequent experiments except otherwise stated.

Additionally, the use of organic solvents and sonication during the PLGA NPs preparation procedure may affect the biological activity of the loaded protein [29]. To protect activity of PE38KDEL, 10% (w/v) trehalose was put into inner water phase as reported before [30]. In our study, the cytotoxic activity of PE38KDEL extracted from PE-NPs

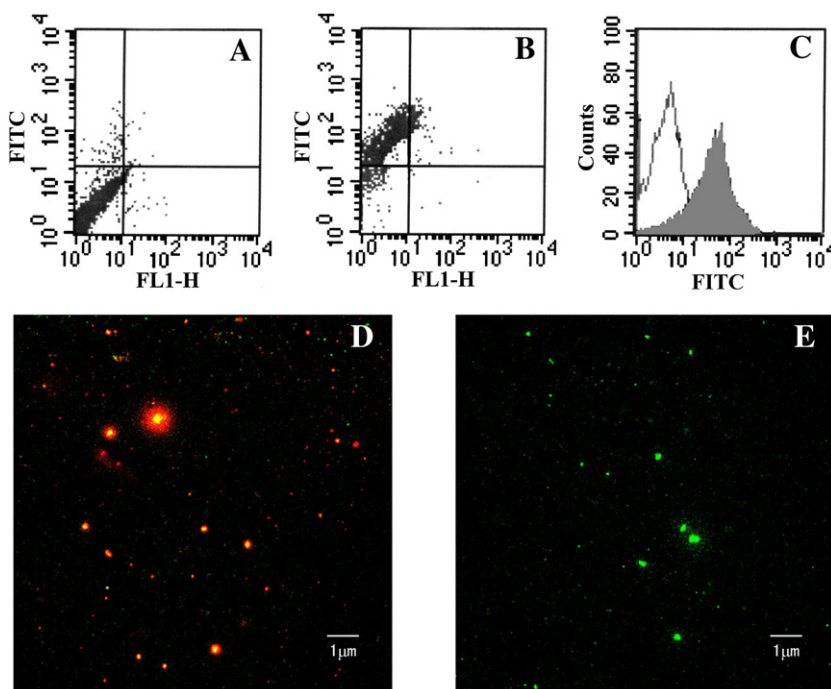


**Fig. 2.** Determination of anti-HER2 Fab' on the surface of nanoparticles by flow cytometric analysis and confocal microscopy. Density plots of antibody modified nanoparticles (A) and antibody modified nanoparticles (B) showed that antibody modified NPs were conjugated with FITC-labeled Fab' and could be distinguished from non-antibody modified NPs by their fluorescence. A shift of FITC fluorescence intensity (C) could be seen for antibody modified NPs (grey histograms) in comparison to non-antibody modified NPs (white histograms), indicating the presence of Fab' on the surface of NPs. Furthermore, confocal microscopic images of FITC-labeled nanoparticles (green) with conjugated phycoerythrin labeled anti-HER2 Fab' (red) showed merged red/green fluorescence (D). The control sample of nanoparticles showed only green fluorescence (E). (For interpretation of the references to colour in this figure legend, the reader is referred to the web version of this article.)

with or without trehalose as the inner water phase was tested in cytotoxicity assay towards BT-474 cells. The results showed that extracted PE38KDEL from PE-NPs with trehalose as the inner water phase retained the similar activity as unencapsulated PE38KDEL [ $IC_{50}$  of  $5.2 \pm 2.2 \mu\text{g/ml}$  vs.  $4.3 \pm 1.6 \mu\text{g/ml}$  for extracted PE38KDEL vs. unencapsulated PE38KDEL, respectively (mean  $\pm$  SD;  $n=3$ )]. However, the activity of extracted PE38KDEL from PE-NPs without trehalose as the inner water phase was greatly reduced [ $IC_{50} = 36.6 \pm 6.9 \mu\text{g/ml}$ , (mean  $\pm$  SD;  $n=3$ )], indicating the activity of PE38KDEL was well-protected by trehalose.

### 3.1.3. Determination of Fab' on the surface of NPs

Binding of anti-HER2 Fab' to the nanoparticle surface was evaluated by flow cytometry (Fig. 2). Unlike the non-antibody modified NPs, the

antibody modified NPs showed green fluorescence, indicating that nearly all NPs are Fab' coated and the population of antibody modified NPs is rather homogeneous.

At the same time, the binding of mAb fragments to the NPs surface was also confirmed by LSCM. As shown in Fig. 2D and E, the antibody modified NPs showed red fluorescence, suggesting NPs were conjugated with Fab'. In contrast, non-antibody modified NPs only showed green fluorescence.

The protein assay was used to quantify the amount of bound Fab' on NPs surface. Since this assay cannot distinguish bound Fab' from PE38KDEL in NPs, PE-NPs were run as a control. According to the protein assay, the amount of conjugated Fab' of antibody modified NPs was shown to be approximately  $19.4 \pm 2.4 \mu\text{g}$  anti-HER2 Fab'/mg NPs (mean  $\pm$  SD;  $n=4$ ).

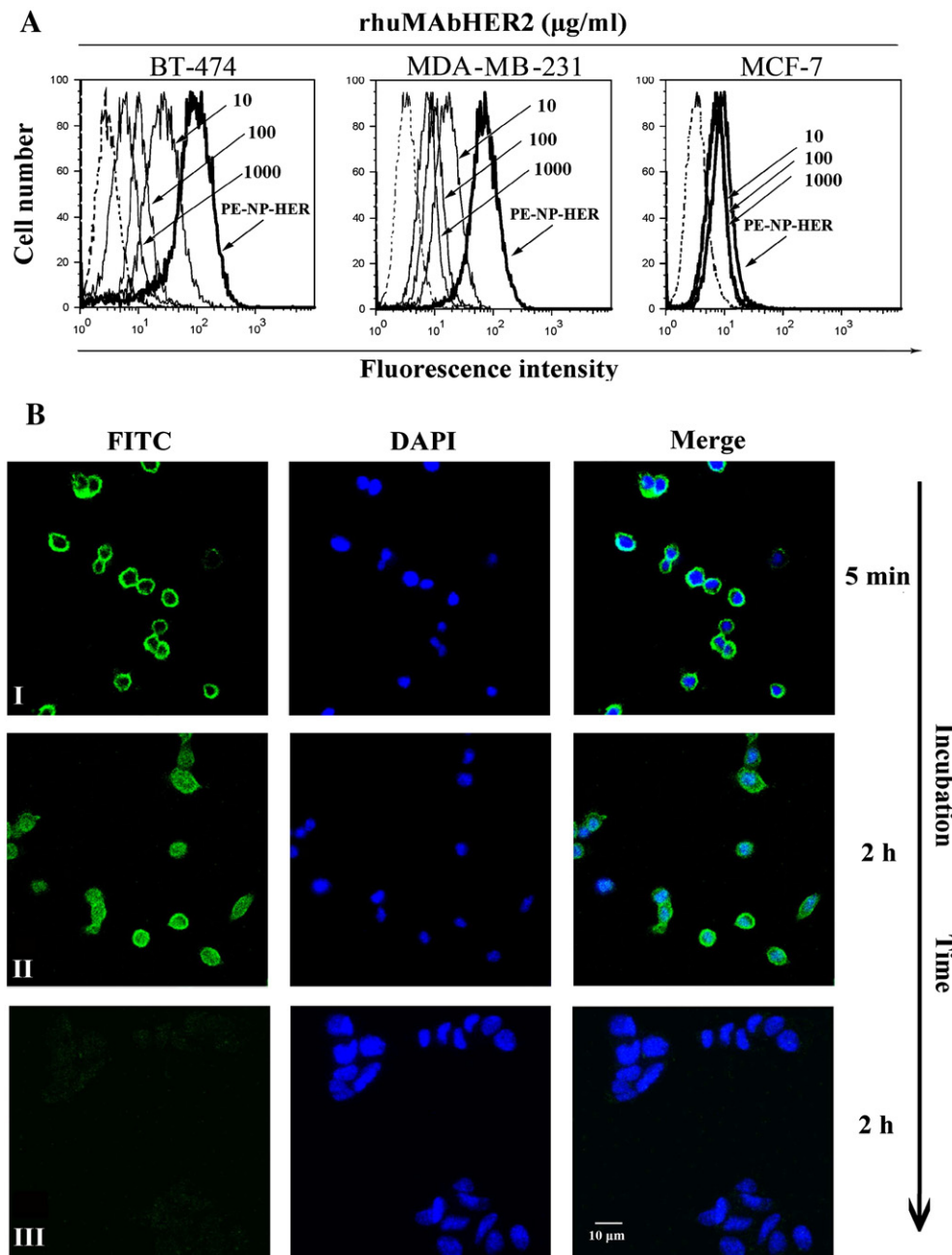


**Fig. 3.** Binding and internalization of antibody modified nanoparticles. (A) Blocking of PE-NPs-HER binding to BT-474, MDA-MB-231 and MCF-7 cells by rhuMabHER2. Cells were incubated with 10, 100, or 1000  $\mu\text{g/ml}$  rhuMabHER2 at  $4^\circ\text{C}$  for 30 min before incubation of the FITC-PE-NPs-HER. Thereafter, cells were assessed by FCM (thin solid line). Untreated cells (dashed line) and cells not treated with rhuMabHER2 (bold line) were used as negative and positive controls, respectively. (B) Binding and internalization analysis of FITC-PE-NPs-HER by confocal laser-scanning microscopy. BT-474 cells: Incubation time 5 min (I) and 2 h (II). MCF-7 cells: Incubation time 2 h (III). Cells were imaged by Leica TCS SP2 Confocal Spectral Microscope (UV-VIS) and the images were analyzed with the Leica Confocal Software. Bar represents 10  $\mu\text{m}$ .

### 3.2. In vitro experiments

#### 3.2.1. Recognition properties of antibody modified NPs

In order to obtain the antibody modified NPs able to target desired cells, the conjugation procedure must preserve the biological activity of targeting ligand. We performed flow cytometry to evaluate the recognition properties of FITC-PE-NPs-HER to HER2 antigen. As shown in Fig. 3, PE-NPs-HER was shown to possess potent binding affinity to HER2-overexpressing BT-474 cells. To confirm the specificity of the interaction of FITC-PE-NPs-HER with the target cells, a competition assay was performed by using free rhuMABHER2. The binding of PE-NPs-HER to BT-474 cells was inhibited by rhuMABHER2 in a dose-dependent manner. Similar results were obtained in other MDA-MB-231 cells. In contrast, the slight binding of PE-NPs-HER observed in MCF-7 cells was not inhibited by rhuMABHER2 and was considered as nearly background. The present data confirmed anti-HER Fab' was effectively conjugated to NPs surface and still preserved its biological activity during the covalent conjugation procedure.

#### 3.2.2. Binding and internalization of antibody modified NPs

To confirm the internalization efficiencies of antibody modified NPs, BT-474 and MCF-7 cells incubated with FITC-PE-NPs-HER were analyzed by laser-scanning confocal microscopy. Internalization of FITC-PE-NPs-HER would lead to cytoplasmically localized green FITC staining. FITC fluorescence was detected only on the BT-474 cell surface after a 5-minute incubation. After a 2 h incubation, FITC fluorescence was detected in the cytoplasm of all cells (Fig. 3). In contrast, when incubated with HER2 negative MCF-7 cells for 2 h, no significantly FITC fluorescence was detected.

#### 3.2.3. In vitro cytotoxicity assays

PE-NPs-HER was tested for cytotoxic activity against BT-474, MDA-MB-231 and MCF-7 cell lines. As shown in Table 2 and Supplementary Fig. 2, BT-474 cells, which expressed high level of HER2 antigens, were most sensitive to PE-NPs-HER ( $IC_{50}=45.86$  pM). MDA-MB-231 cells expressing lower level of HER2 antigens than BT-474 were also sensitive to PE-NPs-HER ( $IC_{50}=265.31$  pM). But the HER2-negative MCF-7 cells were much less sensitive to PE-NPs-HER, with a very high  $IC_{50}$  value ( $IC_{50}>1000$  pM). Similar results were obtained when the three cell lines were incubated with PE-HER, suggesting that the binding ability and specificity of PE-NPs-HER and PE-HER to HER2 antigen were critical for induction of cytotoxicity. It was clearly shown that PE-NPs-HER was more cytotoxic against BT-474 cells when compared with PE-HER ( $IC_{50}$  of PE-NPs-HER being  $45.86\pm 8.69$  pM vs. that of PE-HER being  $98.67\pm 9.59$  pM respectively (mean $\pm$ SD,  $n=3$ );  $P<0.05$ ) (Table 2). The similar results were obtained when MDA-MB-231 cells were used. However, mixture of PE-NPs with free anti-HER2 Fab' as the same amount as it conjugated to PE-NPs-HER showed very high  $IC_{50}$  values for the three cell lines, indicating that the cytotoxicity of PE-NPs-HER was dependent on the conjugated anti-HER2 Fab' but not free anti-HER2 Fab'. Compared with other control groups, PE-NPs-HER showed notably enhanced cytotoxicity against HER2-overexpressing breast cancer cells. We speculated that the antitumor mechanism of PE-NPs-HER is their binding and getting internalized into tumor

cells with subsequent intracellular release of PE38KDEL after PLGA degradation [31].

To eliminate the possibility that anti-HER2 Fab' or NPs formulated with PLGA copolymer system was responsible for the cytotoxicity, we performed similar cytotoxicity assays with NPs and NPs-HER, which did not encapsulate PE38KDEL. Cytotoxicity of NPs and NP-HER without PE38KDEL was evaluated at 2 days at the highest PLGA concentration used in the cytotoxicity assays. Cell viability of NPs and NP-HER was  $97\pm 3\%$  and  $96\pm 2\%$  respectively (mean $\pm$ SD,  $n=3$ ). The results clearly demonstrated the lack of cellular cytotoxicity of these materials due to the absence of PE38KDEL.

### 3.3. In vivo experiments

#### 3.3.1. Nonspecific toxicity assays

In addition to enhanced efficacy, encapsulation of PE38KDEL in either PLGA NPs or anti-HER2 PLGA NPs was associated with markedly reduced host toxicity compared with free PE38KDEL. In studies to determine the MTD in nude mice with tumor xenografts, various doses of PE38KDEL, PE-HER, PE-NPs, or PE-NPs-HER were administered i.v. once a week for three doses. The MTDs of PE-NPs-HER (2.92 mg/kg) and PE-NPs (2.14 mg/kg) were about 2.5-fold greater than those of PE-HER (0.92 mg/kg) and PE38KDEL (0.85 mg/kg).

To evaluate hepatotoxicity of PLGA encapsulated PE38KDEL, we collected blood samples 2 h and 48 h after the administration of drugs at an equivalent dose of 0.5 mg/kg PE38KDEL. The results suggested that there was a significant increase in the level of plasma ALT after the administration of PE38KDEL and PE-HER, whereas no obvious change in the plasma level of ALT was observed after the injection of PLGA encapsulated PE38KDEL (including PE-NPs-HER, PE-NPs combined with anti-HER2 Fab', PE-NPs-anti-CD25) (data not shown). To observe the pathological change of liver, mice were sacrificed 72 h after administration of drugs at an equivalent dose of 0.5 mg/kg PE38KDEL and sections of the livers were prepared and stained with H&E. In the mice treated with PE38KDEL and PE-HER, there were evidences of vasodilatation, hyperemia, and fatty degeneration, whereas the livers from the mice treated with PLGA encapsulated PE38KDEL appeared normal (Supplementary Fig. 3).

One possible explanation for the reduction of nonspecific toxicity of PE38KDEL in both NPs treated groups as compared with the PE38KDEL and PE-HER treated groups may be that encapsulation of PE38KDEL into NPs could avoid the contact of PE38KDEL with receptors specific for protein toxins in normal tissues. Furthermore, compared PE-NPs-HER treated group with PE-NPs treated group, the former is expected to get internalized into tumor cells with subsequent intracellular release. However, the non-antibody modified NPs may release the drug in the extracellular space or other organs, cause systemic distribution, resulting in little more increased nonspecific toxicity than antibody modified NPs.

In this study, PE-NPs-HER had shown to be well tolerated in mice compared with conventional immunotoxin PE-HER, suggesting it may be a novel PE-based antibody modified NPs with much less toxicity for clinical use.

#### 3.3.2. In vivo antitumor study

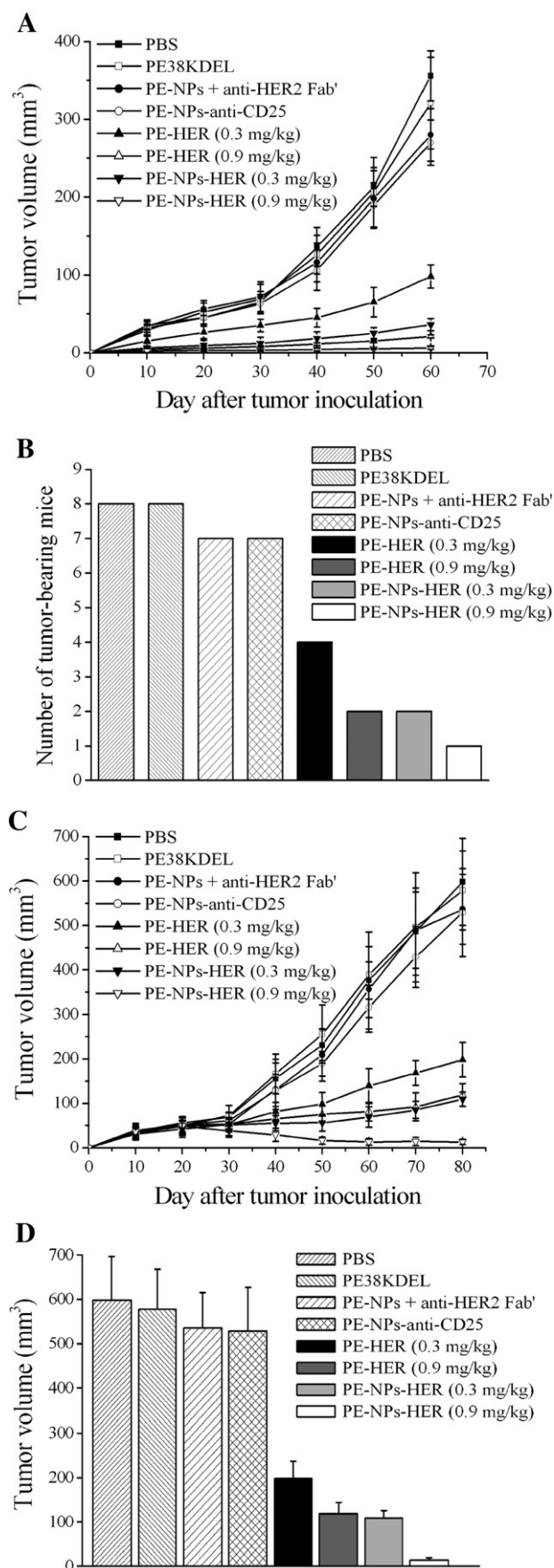
The antitumor efficacy of the bioconjugates was evaluated using xenograft models of breast cancer developed by s.c. injections of BT-474 cells in the back of BALB/c nude mice. As shown in Fig. 4A, in the control groups, treated with PBS, PE38KDEL, PE-NPs combined with anti-HER2 Fab', PE-NPs-anti-CD25, given at doses of 0.9 mg/kg, the tumors grew rapidly, indicating PE38KDEL and non-antibody modified PE38KDEL PE38KDEL-loaded NPs were not effective in suppressing the tumor growth. In contrast, both PE-HER and PE-NPs-HER could significantly inhibit the tumor growth in tumor-bearing mice in a dose-dependent manner. Compared with PE-HER, the antitumor activity of PE-NPs-HER was markedly improved: the final mean tumor

**Table 2**  
 $IC_{50}$  (pM) of various drugs in breast cancer cell lines

	PE-NPs-HER	PE-HER	PE-NPs+ anti-HER2 Fab'	PE-NPs-anti-CD25	PE38KDEL
BT-474	$46\pm 9^a$	$99\pm 10^*$	>1000	>1000	>1000
MDA-MB-231	$265\pm 50$	$327\pm 26^*$	>1000	>1000	>1000
MCF-7	>1000	>1000	>1000	>1000	>1000

<sup>a</sup> Data are expressed as the mean $\pm$ SD ( $n=3$ ).

\*  $P<0.05$ ; comparison of  $IC_{50}$  of PE-NPs-HER and PE-HER in BT-474 or MDA-MB-231 cells showed significant differences using Student's *t* test (two-sample individual *t* test).



load was  $36 \pm 8 \text{ mm}^3$  (0.3 mg/kg) and  $6 \pm 2 \text{ mm}^3$  (0.9 mg/kg), respectively (mean  $\pm$  SD;  $n=8$ , significantly smaller than proportional PE-HER treated group by ANOVA at 99% confidence interval). In PE-NPs-HER treated group, we observed that only 1 and 2 of 8 mice had developed tumors within 60 days, at 0.9 and 0.3 mg/kg respectively. However, there were 2 and 4 mice which developed tumors in proportional PE-HER treated group, indicating that PE-NPs-HER exhibited more potent antitumor activity than immunotoxin PE-HER (Fig. 4B).

In clinical settings, a therapeutic approach on developed tumors is desirable. Therefore, we investigated the effect of PE-NPs-HER on already existing breast cancer. Here (Fig. 4), we could show that, for each control groups of PBS, PE38KDEL, PE-NPs combined with anti-HER2 Fab', PE-NPs-anti-CD25, given at doses of 0.9 mg/kg, the treatment did not show any long-term efficacy, and the mean tumor sizes at the end of the study for the groups were  $598 \pm 98 \text{ mm}^3$ ,  $579 \pm 89 \text{ mm}^3$ ,  $536 \pm 79 \text{ mm}^3$ , and  $529 \pm 99 \text{ mm}^3$ , respectively (mean  $\pm$  SD;  $n=8$ ). In contrast, injection of PE-HER and PE-NPs-HER could substantially slow breast cancer growth in a dose-dependent manner. The 0.3, 0.9 mg/kg PE-HER and 0.3 mg/kg PE-NPs-HER treated groups were also more efficacious than the control groups (the final mean tumor loads of these three groups were all significantly smaller than the control groups by ANOVA at 99% confidence interval), but significantly less efficacious when compared with the 0.9 mg/kg PE-NPs-HER treated group. The 0.9 mg/kg PE-NPs-HER treated group demonstrated the most dramatic efficacy: the final mean tumor load was  $13 \pm 6 \text{ mm}^3$  (mean  $\pm$  SD;  $n=8$ , significantly smaller than all other groups by ANOVA at 95% confidence interval). The study clearly demonstrated the potent antitumor activity of PE-NPs-HER.

We speculated that the high antitumor activity of PE-NPs-HER was achieved by the following mechanisms. Antibody modified NPs delivery involves two phases [32]. In the first phase, NPs slowly accumulate in tumor tissue, ultimately reaching high tumor levels due to the enhanced permeability and retention effect [6]. In the second phase, non-antibody modified NPs remain in the interstitial space and are subject to decomposition, degradation, or phagocytosis, with resulting release of drug. In contrast, antibody modified NPs bind to and internalize in tumor cells via ligand–receptor interactions, resulting a potent antitumor activity to cancer cells. Detailed studies on tissue distribution and cell-binding are under our further study. Taken together, PE-NPs-HER was shown to retain potent antitumor activity but with a remarkable attenuation in nonspecific toxicity, indicating that it might become an effective antitumor agent with much less toxicity for clinical application.

#### 4. Conclusions

PE-based immunotoxins represent a promising therapeutic approach in cancer therapy. Currently, more than 10 PE-based immunotoxins have been in clinical trials [1]. However, the clinical use of PE-based immunotoxins is severely hampered by the

**Fig. 4.** Antitumor study in mice bearing BT-474 breast cancer xenografts. (A) Antitumor effect of various agents in nude mice. Groups of 8 nude mice were s.c. inoculated with  $5 \times 10^6$  BT-474 cells on day 0. Starting on day 1, the mice were treated with PBS, PE38KDEL (0.9 mg/kg), PE-NPs combined with anti-HER2 Fab' (0.9 mg/kg), PE-NPs-anti-CD25 (0.9 mg/kg), PE-HER (0.3 mg/kg), PE-HER (0.9 mg/kg), PE-NPs-HER (0.3 mg/kg) or PE-NPs-HER (0.9 mg/kg) twice daily for three consecutive days. Data are expressed as mean tumor volume  $\pm$  SD ( $n=8$ ). (B) Plot of outcomes for each of the treatment groups. On day 60, the number of tumor-bearing mice of each group was calculated. The bar indicates the number of tumor-bearing mice of each group. Each group consists of 8 nude mice. (C) For therapeutic experiments, tumor growth was induced by s.c. injection of  $5 \times 10^6$  BT-474 cells on the back. After 20 days when the tumor growth was visible (about  $\sim 50 \text{ mm}^3$ ), mice were injected with various agents through the tail vein twice daily for three consecutive days. Tumors were measured with a caliper every 5 days for an additional 60 days and tumor volume was calculated as described above. Data are expressed as mean tumor volume  $\pm$  SD ( $n=8$ ). (D) Plot of outcomes for each of the treatment groups. The bar indicates the tumor volume at the end-point (80 day) of each group. Each group consists of 8 nude mice.

nonspecific toxicity of PE, which is usually characterized by hepatotoxicity. In this study, for the first time, we used biodegradable PLGA polymers, which are commonly applied in encapsulating peptide and protein, to develop small sized PE38KDEL-loaded PLGA NPs. And we also conjugated targeted ligand anti-HER2 Fab' onto the surface of NPs via conjugation to form antibody modified NPs. Although there are many chemotherapeutics-loaded NPs targeting HER2 antigen [33–35], the protein toxin PE loaded NPs modified with anti-HER2 Fab' have not been investigated. Remarkably, the biological activities of PE38KDEL and anti-HER2 Fab' were well well-protected during preparation procedure. *In vitro* experiments demonstrated their potent binding affinity and cytotoxicity to HER2-overexpressing breast cancer cells. Most strikingly, compared with conventional immunotoxin PE-HER, PE-NPs-HER showed increased antitumor activity and decreased nonspecific toxicity. It is conceivable that this novel nanotechnology would be applied in other immunotoxins. This new therapeutic approach might be a useful treatment for HER2-overexpressing breast cancer with fewer side effects than conventional PE-based immunotoxins.

### Acknowledgements

We acknowledge Dr. Wang in Instrumental Analysis Center of Shanghai Jiao Tong University (Shanghai, China) for helpful work of TEM images. This research was supported by National Natural Science Foundation of China, Shanghai Commission of Science and Technology, Ministry of Science and Technology of China (973&863 program projects).

### Appendix A. Supplementary data

Supplementary data associated with this article can be found, in the online version, at doi:10.1016/j.jconrel.2008.03.010.

### References

- [1] I. Pastan, R. Hassan, D.J. FitzGerald, R.J. Kreitman, Immunotoxin treatment of cancer, *Annu. Rev. Med.* 58 (2007) 221–237.
- [2] I. Pastan, R. Hassan, D.J. FitzGerald, R.J. Kreitman, Immunotoxin therapy of cancer, *Nat. Rev., Cancer* 6 (7) (2006) 559–565.
- [3] R.J. Kreitman, Immunotoxins in cancer therapy, *Curr. Opin. Immunol.* 11 (5) (1999) 570–578.
- [4] R. Baluna, E. Coleman, C. Jones, V. Ghetie, E.S. Vitetta, The effect of a monoclonal antibody coupled to ricin A chain-derived peptides on endothelial cells in vitro: insights into toxin-mediated vascular damage, *Exp. Cell Res.* 258 (2) (2000) 417–424.
- [5] C.B. Siegall, D. Liggitt, D. Chace, B. Mixan, J. Sugai, T. Davidson, M. Steinitz, Characterization of vascular leak syndrome induced by the toxin component of *Pseudomonas* exotoxin-based immunotoxins and its potential inhibition with nonsteroidal anti-inflammatory drugs, *Clin. Cancer Res.* 3 (3) (1997) 339–345.
- [6] T.M. Allen, P.R. Cullis, Drug delivery systems: entering the mainstream, *Science* 303 (5665) (2004) 1818–1822.
- [7] P.L. Brannon, J.O. Blanchette, Nanoparticle and targeted systems for cancer therapy, *Adv. Drug Deliv. Rev.* 56 (11) (2004) 1649–1659.
- [8] M.M. Gaspar, D. Blanco, M.E. Cruz, M.J. Alonso, Formulation of L-asparaginase-loaded poly(lactide-co-glycolide) nanoparticles: influence of polymer properties on enzyme loading, activity and in vitro release, *J. Control. Release* 52 (1–2) (1998) 53–62.
- [9] O.C. Farokhzad, J. Cheng, B.A. Teply, I. Sherifi, S. Jon, P.W. Kantoff, J.P. Richie, R. Langer, Targeted nanoparticle-aptamer bioconjugates for cancer chemotherapy in vivo, *Proc. Natl. Acad. Sci. U. S. A.* 103 (16) (2006) 6315–6320.
- [10] O.C. Farokhzad, J.M. Kap, R. Langer, Nanoparticle-aptamer bioconjugates for cancer targeting, *Expert Opin. Drug Deliv.* 3 (3) (2006) 311–324.
- [11] K. Avgoustakis, Pegylated poly(lactide) and poly(lactide-co-glycolide) nanoparticles: preparation, properties and possible application in drug delivery, *Curr. Drug Deliv.* 1 (4) (2004) 321–333.
- [12] A. Ghosh, W.D. Heston, Tumor target prostate specific membrane antigen (PSMA) and its regulation in prostate cancer, *J. Cell. Biochem.* 91 (3) (2004) 528–539.
- [13] Y. Tsutsumi, M. Onda, S. Nagata, B. Lee, R.J. Kreitman, I. Pastan, Site-specific chemical modification with polyethylene glycol of recombinant immunotoxin anti-Tac(Fv)-PE38 (LMB-2) improves antitumor activity and reduces animal toxicity and immunogenicity, *Proc. Natl. Acad. Sci. U. S. A.* 97 (15) (2000) 8548–8553.
- [14] H. Wartlick, K. Michaelis, S. Balthasar, K. Strebhardt, J. Kreuter, K. Langer, Highly specific HER2-mediated cellular uptake of antibody modified nanoparticles in tumour cells, *J. Drug Target.* 12 (7) (2004) 461–471.
- [15] J.W. Park, K. Hong, D.B. Kirpotin, D. Papahadjopoulos, C.C. Benz, Immunoliposomes for cancer treatment, *Adv. Pharmacol.* 40 (1997) 399–435.
- [16] S. Song, J. Xue, K. Fan, Q. Zhou, H. Wang, Y. Guo, Preparation and characterization of fusion protein truncated *Pseudomonas* exotoxin A (PE38KDEL) in *Escherichia coli*, *Protein Expr. Purif.* 44 (1) (2005) 52–57.
- [17] H. Wang, S. Song, G. Kou, B. Li, D. Zhang, S. Hou, W. Qian, J. Dai, L. Tian, J. Zhao, Y. Guo, Treatment of hepatocellular carcinoma in a mouse xenograft model with an immunotoxin which is engineered to eliminate vascular leak syndrome, *Cancer Immunol. Immunother.* 56 (11) (2007) 1775–1783.
- [18] S.E. Lupold, B.J. Hicke, Y. Lin, D.S. Coffey, Identification and characterization of nuclease-stabilized RNA molecules that bind human prostate cancer cells via the prostate-specific membrane antigen, *Cancer Res.* 62 (14) (2002) 4029–4033.
- [19] M. Pegram, D. Ngo, Application and potential limitations of animal models utilized in the development of trastuzumab (Herceptin): a case study, *Adv. Drug Deliv. Rev.* 58 (5–6) (2006) 723–734.
- [20] P. Sapra, T.M. Allen, Ligand-targeted liposomal anticancer drugs, *Prog. Lipid Res.* 42 (5) (2003) 439–462.
- [21] T. Kondo, D. FitzGerald, V.K. Chaudhary, S. Adhya, I. Pastan, Activity of immunotoxins constructed with modified *Pseudomonas* exotoxin A lacking the cell recognition domain, *J. Biol. Chem.* 263 (19) (1988) 9470–9475.
- [22] F.J. Martin, W.L. Hubbell, D. Papahadjopoulos, Immunospesific targeting of liposomes to cells: a novel and efficient method for covalent attachment of Fab' fragments via disulfide bonds, *Biochemistry* 20 (14) (1981) 4229–4238.
- [23] D. Blanco, M.J. Alonso, Development and characterization of protein-loaded poly(lactic/glycolic acid) nanospheres, *Eur. J. Pharm. Biopharm.* 43 (3) (1997) 285–294.
- [24] S.H. Kim, J.H. Jeong, K.W. Chun, T.G. Park, Target-specific cellular uptake of PLGA nanoparticles coated with poly(L-lysine)-poly(ethylene glycol)-folate conjugate, *Langmuir* 21 (19) (2005) 8852–8857.
- [25] T.G. Park, L.H. Yong, N.Y. Sung, A new preparation method for protein loaded poly(D,L-lactic-co-glycolic acid) microspheres and protein release mechanism study, *J. Control. Release* 55 (2–3) (1998) 181–191.
- [26] P. Kocbek, N. Obermajer, M. Cegnar, J. Kos, J. Kristl, Targeting cancer cells using PLGA nanoparticles surface modified with monoclonal antibody, *J. Control. Release* 120 (1–2) (2007) 18–26.
- [27] J. Schümann, D. Wolf, A. Pahl, K. Brune, T. Papadopoulos, N. van Rooijen, G. Tiegs, Importance of Kupffer cells for T-cell-dependent liver injury in mice, *Am. J. Pathol.* 157 (5) (2000) 1671–1683.
- [28] I. Brigger, C. Dubernet, P. Couvreur, Nanoparticles in cancer therapy and diagnosis, *Adv. Drug Deliv. Rev.* 54 (5) (2002) 631–651.
- [29] I.T. Degim, N. Celebi, Controlled delivery of peptides and proteins, *Curr. Pharm. Des.* 13 (1) (2007) 99–117.
- [30] M. Wolf, M. Wirth, F. Pittner, F. Gabor, Stabilisation and determination of the biological activity of L-asparaginase in poly(D, L-lactide-co-glycolide) nanospheres, *Int. J. Pharm.* 256 (1–2) (2003) 141–152.
- [31] Y. Mo, L.Y. Lim, Preparation and in vitro anticancer activity of wheat germ agglutinin (WGA)-conjugated PLGA nanoparticles loaded with paclitaxel and isopropyl myristate, *J. Control. Release* 107 (1) (2005) 30–42.
- [32] C. Mamot, D.C. Drummond, C.O. Noble, V. Kallab, Z. Guo, K. Hong, D.B. Kirpotin, J.W. Park, Epidermal growth factor receptor-targeted immunoliposomes significantly enhance the efficacy of multiple anticancer drugs in vivo, *Cancer Res.* 65 (24) (2005) 11631–11638.
- [33] J.W. Park, K. Hong, D.B. Kirpotin, G. Colbern, R. Shalaby, J. Baselga, Y. Shao, U.B. Nielsen, J.D. Marks, D. Moore, D. Papahadjopoulos, C.C. Benz, Anti-HER2 immunoliposomes: enhanced efficacy attributable to targeted delivery, *Clin. Cancer Res.* 8 (4) (2002) 1172–1181.
- [34] T. Yang, M.K. Choi, F.D. Cui, J.S. Kim, S.J. Chung, C.K. Shim, D.D. Kim, Preparation and evaluation of paclitaxel-loaded PEGylated immunoliposome, *J. Control. Release* 120 (3) (2007) 169–177.
- [35] J.W. Park, D.B. Kirpotin, K. Hong, R. Shalaby, Y. Shao, U.B. Nielsen, J.D. Marks, D. Papahadjopoulos, C.C. Benz, Tumor targeting using anti-her2 immunoliposomes, *J. Control. Release* 74 (1–3) (2001) 95–113.